6-10-2015

Tracking of Spall Deterioration on Tapered Roller Bearings

Amy Gonzalez

Constantine Tarawneh

Ping Hu

Joseph A. Turner

Brent Wilson

DRAFT

Proceeding of the ASME 2015 Joint Rail Conference
JRC2015
March 23-26, 2015, San Jose, CA, USA

JRC2015-5793

TRACKING OF SPALL DETERIORATION ON TAPERED ROLLER BEARINGS

Amy Gonzalez
Department of Mechanical Engineering
University of Texas-Pan American
Edinburg, TX 78539, USA
agonzalezx@broncs.utpa.edu

Constantine Tarawneh
Department of Mechanical Engineering
University of Texas-Pan American
Edinburg, TX 78539, USA
tarawneh@utpa.edu

Ping Hu and Joseph A. Turner
Dept. of Mechanical and Materials Engineering
University of Nebraska-Lincoln
Lincoln, NE 68588, USA
jaturner@unl.edu

Brent M. Wilson
Amsted Rail Company
Granite City, IL 62040, USA
bwilson@amstedrail.com

ABSTRACT

Fatigue spall initiation is one of the major modes of premature bearing failure. The spall initiation is often exacerbated by the presence of impurities in the near-surface region (~400 μm) of the bearing raceways. Once a spall initiates, it can propagate rapidly, leading to abnormal bearing operation and possible catastrophic failure if not detected early. Testing performed at the University of Texas-Pan American (UTPA) has focused on ultrasonically scanned tapered roller bearings found to have inclusion content within 400 μm of the surface of the raceways. These bearings undergo accelerated service life tests in which spall initiation is detected and tracked over time while documenting spall growth. The work presented here provides several study cases that document the spall initiation and propagation on ultrasonically scanned tapered roller bearing components. Results show that spalls generally initiate on locations corresponding to sites of sub-surface inclusions, and they grow many times their original size within relatively short operating periods. The study also shows that spalls tend to initiate and propagate at a faster rate on bearing cups (outer rings) than on cones (inner rings).

INTRODUCTION

Tapered-roller bearings are commonly used in freight railcar operation. The bearings are comprised of two inner rings (cones) and one outer ring (cup) with the rollers transferring the load between the two components. In an operational setting, a side-frame is placed over two bearings distributing one-fourth of the load of the railcar between the two. Because the cups are fixed in place, the top hemisphere of the cup is always loaded. This region is referred to as the "loaded zone". Unlike the cups, the cones are continuously rotating in unison with the wheel and axle set, which allows the cones to undergo cyclic loading as regions enter and exit the loaded zone.

One of the most common causes of railroad tapered-roller bearing failure is due to rolling contact fatigue (RCF), which can lead to spalling. Spalling typically occurs on the rolling surfaces of bearings, otherwise known as raceways, due to the presence of subsurface inclusions. Effects of RCF on sites of subsurface inclusions and how the surface of the steel is affected have been thoroughly investigated [1-6]. According to Hertzian contact mechanics, the highest principal stresses occur at the surface, but are compressive in nature [7]. However, maximum shear stress exists below the rolling surface due to contact loading. This stress, which initiates fatigue, reaches a maximum beneath the surface based on the geometry of the two raceways. For example, RCF regions in cup and cone raceways reach maximum shear stresses at approximately 200 μm below the contact surface [7]. Subsurface inclusions located in this area act as stress concentration sites which tend to initiate fatigue cracking. Once these cracks reach the surface of the bearing raceway, metal begins to flake off, leaving behind a cavity known as a "spall." Subsurface inclusions are generally composed of oxides or other non-metallics caught in the steel during manufacturing. Various types of inclusions have proven to have different effects on the micro-cracking that occurs within steel when exposed to RCF [8]. While it is nearly impossible to manufacture a steel product with the absence of inclusions, it is the quantity, distribution, location, and size of inclusions that determines the fatigue life of a product [9].

The moment a spall initiates, metallic debris is introduced into the bearing lubricant, allowing that debris to become caught between the bearing's dynamic components, which results in the sliding or skidding of the rollers as opposed to pure rolling. When rollers begin to slide, they cause excessive frictional heating within the bearing, which can then cause the lubricant to break down, increasing the bearing temperature even further. The effects of slipping and sliding of rolling components on contact surfaces is further discussed in [10]. There have been a few attempts by researchers to correlate bearing life to contact fatigue and subsurface inclusions [11, 12]. Some have even attempted to increase the longevity of bearing life by utilizing a method involving Hot Isostatic Pressing (HIP) [13]. The work presented here investigates the effects of the presence of subsurface inclusions on bearing cup and cone raceways, and how rapidly a spall initiates and progresses under service life operating conditions.

For this study, new bearing components (cups and cones) were scanned using ultrasonic (UT) surface wave scanning to detect and identify potentially destructive subsurface inclusions present in the RCF regions of the rolling surfaces. Three service life tests of these components were performed. The first of which examined the effects of subsurface inclusions present within 200 µm beneath the surface of cone raceways. The second service life test was carried out to explore the effects of subsurface inclusions within 200 µm beneath the surface of cup raceways. In the third service life test, the effects of subsurface inclusions present within 200, 300, and 400 µm beneath the cup raceways were studied. This paper summarizes the main outcomes of the third service life test carried out on ultrasonically scanned bearing components, and emphasizes the importance of bearing steel cleanliness.

SELECTION OF BEARING COMPONENTS FOR SERVICE LIFE TESTING

A total of one hundred and six bearing cups and forty cones were ultrasonically scanned at Amsted Rail's Bearing Division, BRENCO, out of which twelve cones and thirteen cups were selected for possible service life testing. The chosen components were then shipped and rescanned at the University of Nebraska-Lincoln (UNL) to validate BRENCO's results, and identify any inclusions that may have been missed by the initial scanning. The inspection volume of the of the material surface varied between 200, 300, and 400 µm, which are calculated using the testing frequencies 15, 10, and 7.5 MHz, respectively, and the Rayleigh wave speed. The components for the first two service life tests were only scanned with the 15 MHz transducer, while the components of the third service life test were ultrasonically scanned at depths of 200, 300, and 400 µm corresponding to the 15, 10, and 7.5 MHz transducers, respectively.

The results from the UT surface wave scanning performed at UNL on the cups used in the third service life test are summarized in Table 1. This table lists the locations of the subsurface inclusions identified on a select few of the components. These select few include the components that spalled during service life testing. The locations of the inclusions are in reference to their circumferential (θ) and vertical (z) position. For the cups of the third service life test, the θ-location for the inboard (IB) and outboard (OB) raceways is referenced in Figure 1(a), whereas, the z-location is referenced from the ends of the flat portion in the middle of the cup (where the spacer ring resides) in the axial direction for both the IB and OB raceways as shown in Figure 1(b).

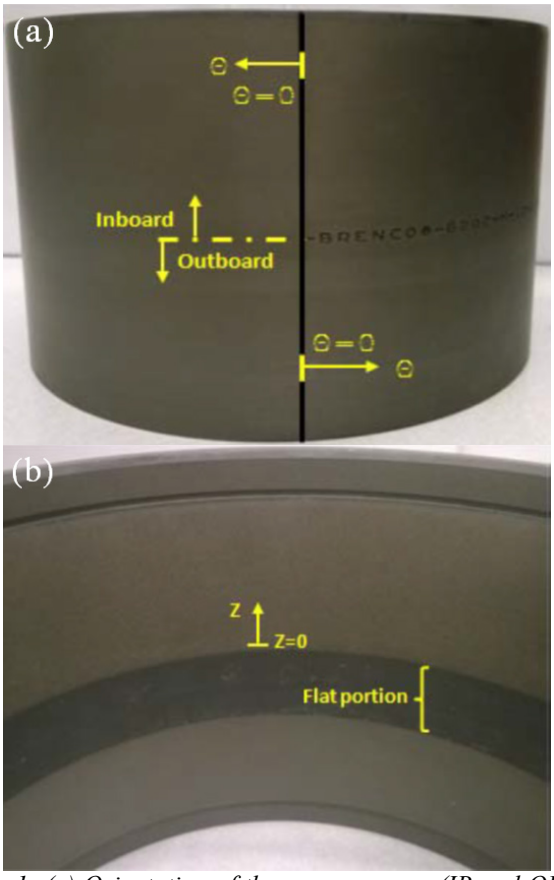

Figure 1: (a) Orientation of the cup raceways (IB and OB) and their respective positive θ rotations, and (b) origin z-coordinate and its positive direction for both IB and OB raceways for the third cup service life test

An example of the UT surface wave scan performed at UNL is provided in Figure 2. The x-direction of the scan represents the circumferential θ-position of the raceway (inboard or outboard) in degrees (°), and the y-direction represents the z-location in millimeters (mm). The high amplitude indications along the bottom of the UT scan image in Figure 2 should be neglected as they represent the onset of the flat portion depicted in Figure 1(b). Note that, defect-free cups were used in the first service life test, and defect-free cones were used in the second and third service life tests. This was done in an effort to confine any possibility of premature failure to the bearing components that contained subsurface inclusions within the raceways.

Table 1: Locations of high amplitude inclusions as detected from the UT surface wave scanning – 15, 10 and 7.5 MHz (cup service life test performed in 2014)

Test Cup	Race (IB/OB)	15 MHz		10 MHz		7.5 MHz	
		θ (°)	z (mm)	θ (°)	z (mm)	θ (°)	z (mm)
A	IB	-	-	-	-	103.934	42.719
	OB	253.034	7.205	251.95	10.158	252.935	12.598
	OB	261.746	7.228	260.567	9.71	261.466	12.236
B	IB	85.939	8.215	85.95	1.266	89.537	8.699
	OB	-	-	-	-	-	-
C	IB	152.259	20.755	154.962	20.189	156.724	21.735
	OB	25.056	28.722	23.25	29.19	22.625	30.896
	OB	153.742	20.218	151.639	20.718	151.306	22.319

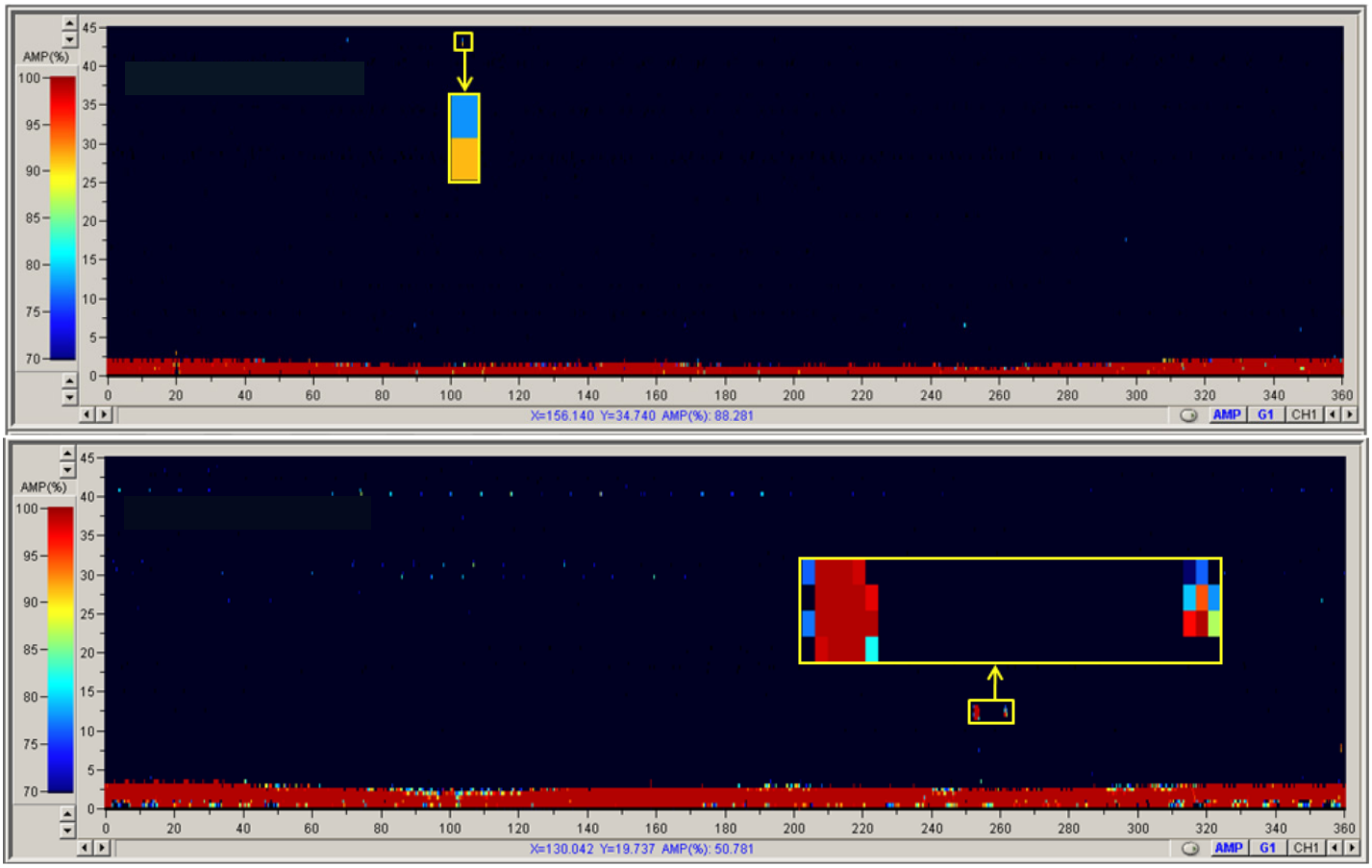

Figure 2: Ultrasonic (UT) wave scan images of Test Cup A, which indicate the presence of three high amplitude subsurface inclusions detected on the IB raceway (top) and OB raceway (bottom) – 7.5 MHz transducer (400 µm depth from raceway surface)

Rollers and other bearing components were not scanned for subsurface inclusions. In total, eight cones and seven cups were used to carry out the three consecutive service life tests utilizing a dynamic four-bearing test rig at the University of Texas-Pan American (UTPA). The work presented in this paper will mainly focus on the UT surface wave scanned components that spalled during the third service life test and their spall progression upon further testing. An in-depth overview of the first two service life tests can be found elsewhere [14, 15].

EXPERIMENTAL SETUP & INSTRUMENTATION

A dynamic four-bearing test rig at UTPA, pictured in Figure 3, was utilized to perform the service life tests. The dynamic tester can accommodate four Class K (6 ½ × 9 in.) tapered-roller bearings which are mounted on a customized test axle. The bearings are labeled 1 to 4, in increasing order from the pulley to the end cap (refer to Figure 3). By changing the size of the pulley on the motor, the axle can rotate at four various angular velocities which are 498, 562, 618, and 794 r/min, which correspond to train speeds of approximately 53, 60, 66, and 85 mph, respectively. Two large industrial fans provided cross-flow over the test axle to simulate the airflow created by a moving train. The dynamic bearing test rig utilizes a hydraulic cylinder which can apply loads ranging from 0 to 175% of full load with full load being 34,400 lb (100% load) per AAR standard for Class K bearings. The service life test was accelerated by running the bearings at 85 mph and 125% of full load for the majority of the test duration. In an effort to avoid overloading the motor, 17% of full-load (corresponding to the weight of an empty railcar) was used in cold starts when the bearing grease has a higher viscosity.

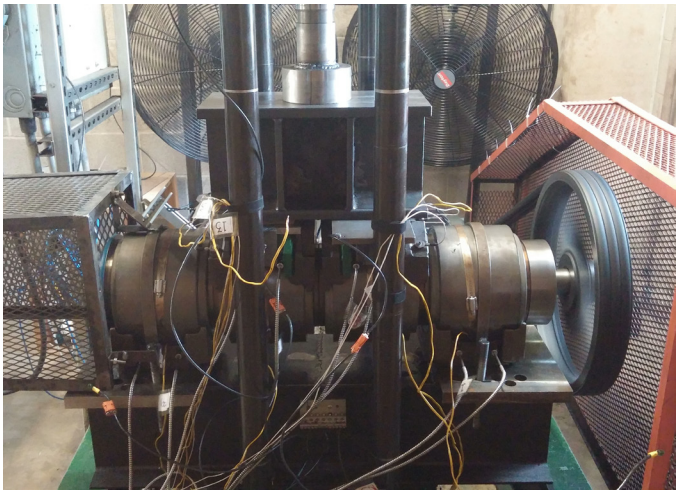

Figure 3: Photograph of the four-bearing dynamic tester at UTPA

The instrumentation setup is shown in Figure 3. Four Class K bearing adapters were machined to house an accelerometer and two bayonet thermocouples, one IB and one OB. K-type bayonet thermocouples and 500g accelerometers were used to monitor and record temperature and vibration of each bearing, respectively. To ensure the accuracy and reliability of the bayonet thermocouples, one K-type thermocouple was affixed to the center of each bearing cup, in line with the two bayonet thermocouples, using a hose clamp. In addition to the thermocouples monitoring bearing temperature, two K-type thermocouples were used to monitor and record the ambient temperature surrounding the dynamic bearing tester.

A LabVIEW™ operated National Instruments (NI) data acquisition system (DAQ) was employed to sample and collect data from the sixteen thermocouples and four accelerometers. A reflective strip was adhered to the end-cap of Bearing 4 so that a tachometer could be used to monitor the speed (r/min) of the axle to allow for accurate mileage calculations. All data acquired from the service life tests was analyzed utilizing the mathematical software MATLAB™.

EXPERIMENTAL PROCEDURES

For the first service life test, the eight cones and four cups shipped from UNL were built into four bearings and mounted onto the axle following a setup similar to the one pictured in Figure 3. The three ultrasonically scanned cups and eight defect-free (control) cones from UNL for the second service life test were assembled and pressed onto the axle following the same exact setup.

For the third service life test, of the ten cups ultrasonically rescanned at UNL, seven were shipped to UTPA along with ten control (defect-free) cones, which were used to build the bearings for this service life test. The setup of the bearings for the third service life test is depicted in Figure 3.

In all service life tests consisting of UT surface wave scanned cups (outer rings), cups having a single inclusion were positioned so that the specific inclusion would be located in the region of maximum applied load (12 o'clock) within the loaded region of the cup. In cases where the test cup contained multiple subsurface inclusions, the inclusion with the highest amplitude indication was positioned directly under the region of maximum applied load (12 o'clock).

Subsequent to the completion of the instrumentation setup of the bearings, load was applied by means of the hydraulic cylinder. The DAQ was then initiated, and the motor was started. Once the break-in period (17% load at 53 mph) was achieved, the load setting and speed were increased to 125% of full-load and 85 mph, respectively.

The developed test plan for the service life tests was to allow the bearings to run uninterrupted while the temperature and vibration signatures of the four bearings were monitored and recorded. If any sudden abnormal behavior was observed in the temperature history or vibration signal of the bearings, the test was stopped to perform a complete teardown, disassembly, and thorough inspection of the bearings in question. Following the detailed inspection, the bearings are rebuilt, total mileage is recorded, and the test is resumed. The described process was to be repeated until the bearings have reached a total operating distance of 250,000 miles, which is the general benchmark established for simulated service life testing. Depending on the number of performed teardowns and inspections, a typical service life test can take anywhere from 6 to 9 months to complete.

EXPERIMENTAL RESULTS

Following the cup service life test performed in 2012, four more cups were ultrasonically scanned and sent to UTPA for the 2014 service life test. As in the previous service life tests,

throughout the duration of this test, the temperature and vibration of all four bearings were closely monitored for any signs of abnormal behavior. An initial teardown and inspection of all bearings was carried out after about 21,000 miles of operation to ensure that all bearings were still free of any defects. The first sign of abnormal operation was observed in Bearing 3 (Test Cup A) after running a total of 51,420 miles. Note that

Upon teardown and inspection of Bearing 3, a spall was discovered on the IB raceway of Test Cup A, as shown in Figure 4. The total spall area was calculated to be approximately 0.175 in.^{2}. The spall formed at a location θ = 104° and z = 43 mm, which coincided with an inclusion listed in Table 1 for Test Cup A. Interestingly, the high amplitude indication of the subsurface inclusion as detected by UT surface wave scans at 7.5 MHz (400 µm) was not detected at 15 and 10 MHz (200 and 300 µm, respectively). As previously mentioned at the beginning of this paper, cups and cones reach maximum shear stress 200 µm beneath their contact surfaces [7], yet this spall initiated at an inclusion site 400 µm beneath the contact surface of the inboard (IB) raceway of Test Cup A, signifying that inclusions at depths below the maximum shear stress region can initiate spalls.

Figure 4: Photograph of spall formation discovered on the IB raceway of Test Cup A after 51,420 miles of operation – 2nd Teardown

Visual inspection of the other three bearings provided no evidence of defects or spalls. All bearings were then rebuilt and pressed onto the axle following the exact setup prior to the first teardown, and service life testing resumed. Upon continuation of the test, Bearing 3 (Test Cup A) exhibited signs of possible spall deterioration or development, which called for a third teardown and inspection to be conducted.

Subsequent to stopping the tester and pressing off the bearings, Bearing 3 was disassembled after running a total of 63,678 miles. Visual inspection of Bearing 3 revealed deterioration of Spall 1 (depicted in Figure 5), which was previously discovered during the second teardown inspection. After only 12,258 miles of additional operation, the spall had expanded along the entire width of the raceway for a total spall area of about 1.050 in.^{2}; i.e., the spall grow in size six times its original area.

Figure 5: Photograph of degradation of the existing spall found on Test Cup A after running an additional 12,258 miles – 3rd Teardown

Visual inspection of the other bearings did not provide evidence of any defects. Once again, the bearings were rebuilt, pressed onto the test axle in the same order as they were before the teardown, and the test resumed. Bearing 3 was closely monitored for any indications of further spall degradation. Shortly after the third teardown (77,506 miles of total operation), Bearing 3 exhibited signs of degradation, which prompted a fourth teardown and visual inspection of all bearings.

Upon teardown and inspection of all bearings, it was found that Spall 1 of Bearing 3 had drastically deteriorated and covered about 4.418 in.^{2} of raceway area, as can be seen in Figure 6. Hence, after only 26,086 miles of additional operation since the second teardown, the spall grew approximately 25 times its original size, from an area of 0.175 in.^{2} to 4.418 in.^{2}. The drastic growth rate of this spall provides clear evidence of the detrimental effect of subsurface inclusions and the importance of bearing steel cleanliness.

Additionally, visual inspection of Test Cup A also revealed the existence of a second spall (Spall 2) on the outboard (OB) raceway, pictured in Figure 7. The position of Spall 2 was located at $\theta \approx 262°$ and $z \approx 7$ mm, which matched exactly the location of a subsurface inclusion detected by the ultrasonic surface wave scanning, listed in Table 1. Spall 2 seems to be at the early stages of spall initiation with a total area of about 0.0734 in.^{2}. However, based on the severe damage exhibited by Test Cup A, it was removed from this service life test to prevent possible catastrophic bearing failure, and was replaced with a control (defect-free) cup. Visual inspection of the other bearings revealed no signs of any spall initiation.

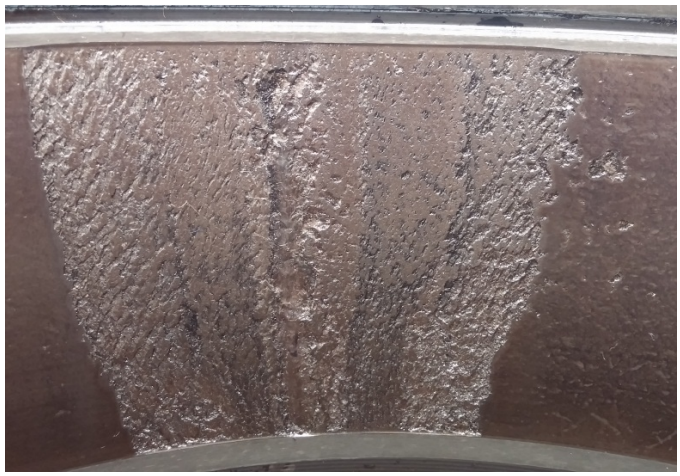

Figure 6: Photograph of further deterioration of Spall 1 on Test Cup A after operating an additional 13,828 miles — 4th Teardown

Figure 7: Photograph of a second spall (Spall 2) that developed on the OB raceway of Test Cup A of Bearing 3 after a total of 77,506 miles of operation – 4th Teardown

Following the completion of inspections, the bearings were rebuilt and mounted onto the test axle. Since Bearing 3 was removed from this service life test and replaced with a defect-free control bearing, a new bearing arrangement was implemented. The two control bearings were mounted as Bearings 1 and 4, whereas, the bearing that previously occupied the Bearing 4 position prior to the teardown was now placed in the Bearing 3 spot, and Bearing 2 maintained its original place on the test axle. The aforementioned bearing re-arrangement was performed in order to place the two test cups containing subsurface inclusions in the middle two spots on the test axle where the bearings are top-loaded as opposed to the two end spots which are bottom-loaded.

Once the setup and instrumentation were completed, the service life test was restarted and the temperature and vibration signatures of the bearings were closely monitored for any signs of spall development. After a total of 174,448 miles of operation, Bearing 3 exhibited signs of abnormal behavior, which triggered a fifth teardown.

Upon teardown and inspection, a newly developed spall was discovered on the IB raceway of Test Cup B of Bearing 3, pictured in Figure 8. The dents observed to the left of the spall (direction of rotation) are most likely caused by the debris from the formed spall. Due to the severity of the dents, they were considered as part of the spall area which was measured as 0.669 $in.^2$. The position of the spall on the IB race was located at $\theta = 86°$ (measured from the center of the deepest region of the spall) and $z > 45$ mm, which did not coincide with any of the subsurface inclusion locations detected by the UT surface wave scans as listed in Table 1 for Test Cup B. However, it should be noted that the ultrasonic surface wave equipment at UNL can only scan up to $z = 45$ mm, leaving the remaining top 5 mm portion of the raceway unscanned. The latter implies that there is a possibility that a subsurface inclusion existed in the region where the spall initiated, but since the surface wave scans do not cover the top portion of the raceway, this inclusion was not identified. Efforts are underway to ensure that the entire cup raceway can be scanned for future testing.

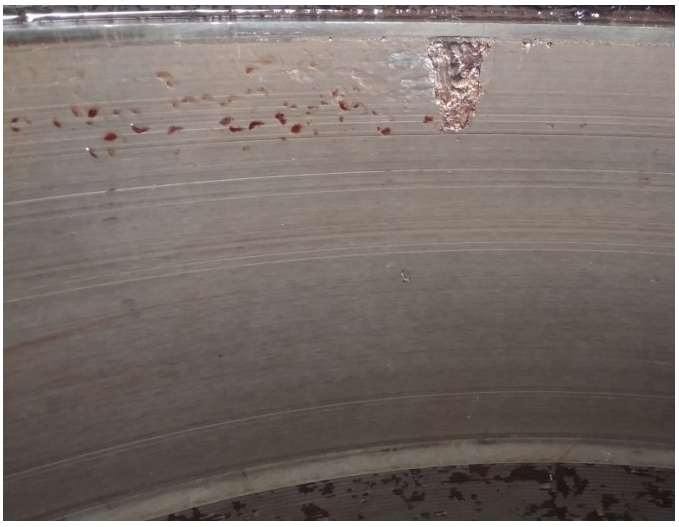

Figure 8: Photograph of a spall that developed on the IB raceway of Test Cup B of Bearing 3 following 174,448 miles of operation – 5th Teardown

Visual inspection of Bearing 2 revealed no evidence of spalling. Subsequent to the completion of the inspections, the bearings were reassembled, and at this point in time, UTPA received two more ultrasonically scanned bearings which replaced the two control bearings (Bearings 1 and 4) used in the setup prior to the fifth teardown. The bearings were pressed onto the test axle, and the test was resumed. Again, the temperature and vibration signatures of all bearings were closely monitored for any abnormal behavior with special attention to Bearing 3 (Test Cup B) which developed the spall seen in Figure 8. After only 10,757 miles of additional operation (185,205 miles of total operation), Bearing 3

exhibited signs of spall deterioration which prompted a sixth teardown.

Following teardown, visual inspection of Bearing 3 revealed noticeable deterioration of the existing spall previously discovered on the IB raceway of Test Cup B, as can be seen in Figure 9. The spall has grown in size and it is accompanied by numerous indentations along the width of the raceway. The spall size is now approximately 2.600 $in.^2$, which means that the initial spall that developed on Test Cup B has grown four times its original size after running an additional 10,757 miles.

Figure 9: Photograph of the deterioration of the existing spall discovered on Test Cup B of Bearing 3 after running an additional 10,757 miles – 6th Teardown

Inspection of the other bearings provided no signs of defects or spalling. The bearings were rebuilt and mounted onto the test axle following the same exact setup as that prior to the sixth teardown, and the test was resumed. Shortly after, Bearing 3 exhibited signs of deterioration which triggered a seventh teardown. At this point, Bearing 3 had run a total of 189,974 miles or operation (i.e. only 4,769 miles of additional operation since the last teardown).

Upon inspection of Bearing 3, the existing spall on Test Cup B was observed to have further degraded, as depicted in Figure 10. The indentations increased in frequency and severity and spanned over a significant portion of the inboard (IB) raceway. The total spall area including all regions of severe indentations was calculated to be 8.292 $in.^2$, which is approximately 3.2 times the previous spall area (measured after the sixth teardown) after only running an additional 4,769 miles, and about 12.4 times the original spall size (measured after the fifth teardown) after operating an additional 15,526 miles. The abovementioned spall growth rates demonstrate how fast spalls can deteriorate once they have initiated, which highlights the importance of bearing steel cleanliness.

Based on the severity of the spall degradation on Test Cup B, Bearing 3 was removed from this service life test and was replaced with another ultrasonically scanned cup sent from UNL. Inspection of the other three bearings did not indicate the presence of any other spalls. Hence, the bearings were rebuilt, pressed onto the test axle, and the test was resumed. After running a total of 214,452 miles, Bearing 2 (Test Cup C) exhibited slight indications of abnormal operation, which called for an eighth teardown.

Figure 10: Photograph of further degradation of the existing spall found on IB raceway of Test Cup B of Bearing 3 following an additional 4,769 miles of operation – 7th Teardown

Visual inspection of Bearing 2 revealed the presence of two spalls on the IB raceway of Test Cup C. The two spalls are connected by two crack lines on either edge of the widths of the spalls, as pictured in Figure 11. Similar to the spall discovered on Test Cup B in the fifth teardown, each of the two spalls was accompanied by dented regions caused by the debris from the formed spalls being wedged between the raceway and the rollers. The total spall area was calculated to be approximately 1.880 $in.^2$. The position of the developed spall is at a location $333° < \theta < 337°$, and $0 < z < 33$ mm. According to Table 1, the spall location did not coincide with any of the listed subsurface inclusion locations for Test Cup C. It is possible that this spall developed on a site of subsurface inclusion that lies deeper than 400 μm.

Figure 11: Photograph of the spall that developed on the IB raceway of Test Cup C of Bearing 2 after running a total of 214,452 miles – 8th Teardown

Visual inspection of the other three bearings provided no evidence of spalls or defects. Once all visual inspections were completed, bearings were rebuilt and mounted onto the test axle following the exact setup as that used prior to the eighth teardown, and the test was continued. Bearing 2 (Test Cup C)

was closely monitored for any unusual behavior that would indicate that the spall has worsened.

After 7,805 additional miles of operation (222,257 miles of total operation), the service life test was stopped and a ninth teardown ensued. Upon visual inspection of Bearing 2 (Test Cup C), it was found that the previously developed spall had deteriorated and was accompanied by regions of severe indentations, as shown in Figure 12. The indentations were observed on the left side of the spall, which is consistent with the axle rotation. The spall area including the regions of severe indentations was measured to be roughly 4.044 in.^{2}, which is about 2.2 times the original spall area.

Figure 12: Photograph of the deterioration of the existing spall located on the IB raceway of Test Cup C after an additional 7,805 miles of operation – 9th Teardown

Visual inspection of the other three bearings did not indicate the presence of any other defects or spalls. The bearings were rebuilt, mounted onto the test axle, and the test was resumed. This time, the bearing previously occupying the Bearing 2 spot was switched with the bearing occupying the Bearing 3 spot, and vice versa. Once again, the bearings were run until the temperature and vibration signatures indicated an abnormal activity.

After running a total of 250,059 miles, Bearing 3 (Test Cup C) exhibited further signs of deterioration, which prompted a tenth teardown. Upon disassembly and inspection of Bearing 3 (formerly Bearing 2), it was observed that the spall deterioration was drastic, as pictured in Figure 13. The degraded spall encompassed nearly half of the loaded region of the IB raceway of Test Cup C. The total spall area measured roughly 8.986 in.^{2}, which means that this spall grew about 2.2 times its size from the previous teardown after 27,802 miles of operation, and approximately 4.8 times its original size (8th teardown) in the span of 35,607 miles of operation. Based on the severity of the spall, and since the bearing reached the 250,000 milestone, it was removed from this service life test and was replaced by another ultrasonically scanned test cup recently received from UNL. This service life test is currently ongoing with four new ultrasonically scanned test cups.

Figure 13: Photograph of the extensive spall degradation of the existing spall found on Test Cup C (Bearing 3) after running an additional 27,802 miles of operation – 10th Teardown

CONCLUSIONS

The results of the three performed service life test studies indicate that, in general, bearing components containing subsurface inclusions have relatively shorter lifespans than their counterparts that have no near-race (within 400 μm) inclusions present. Moreover, subsurface inclusions present within bearing cups (outer rings) seem to initiate spalls more rapidly than subsurface inclusions present in bearing cones (inner rings). The main conclusions from this study are summarized hereafter.

Of the eight cones tested in the first service life test (see Ref [14]), three developed spalls at sites of indicated subsurface inclusions as detected by UT surface wave scanning within the 250,000-mile benchmark usually set in simulated service life testing.

Of the thirteen cups involved in the second and third service life tests, six formed spalls or pits within the 250,000-mile benchmark, and of those six, four of them initiated spalls at indicated subsurface inclusion sites.

The earliest spall to initiate on a cone (inner ring) containing subsurface inclusions occurred after the bearing had ran a total of 198,692 miles [14]. On the contrary, the test cups (outer rings) containing subsurface inclusions initiated spalls as early as 71,954 miles of operation in the second service life test [15], and 51,420 miles of operation in the third service life test. The fact that bearing cups can be positioned such that the subsurface inclusions fall directly under the maximum applied load, whereas, the cones are constantly rotating in and out of the loaded region is one factor that contributes to the aforementioned results.

The results of the service life tests also demonstrate the rapid growth rates of spalls once they have initiated. Evidence of the latter is clearly demonstrated in the case of Test Cup A where the spall that initiated on a site of subsurface inclusion grew in size approximately 25 times its original area in the span of 26,086 miles. The final spall size of Test Cup A is large enough to cause significant heating in the bearing, which, in

extreme cases, could lead to catastrophic bearing failure and possible train derailment.

Finally, the performed service life tests provided clear evidence of the detrimental effects of subsurface inclusions and highlighted the importance of bearing steel cleanliness. Note that, higher quality steel does not ensure the absence of subsurface inclusions nor does it guarantee that those inclusions will not land in an RCF zone. Therefore, the use of novel quality control techniques such as ultrasonic surface wave scanning can help identify bearing components containing subsurface inclusions, which will reduce the number of bearing failures associated with early spall initiation and degradation. The latter will contribute to safer and much improved railroad operations.

ACKNOWLEDGMENTS

Special thanks to the Amsted Rail Company for funding all aspects of this research. The project is a collaborative effort between Amsted Rail's Bearing Division, BRENCO, the University of Texas-Pan American (UTPA), and the University of Nebraska-Lincoln (UNL).

REFERENCES

[1] I. El-Thalji, E. Jantunen, "A Descriptive Model of Wear Evolution in Rolling Bearings," in Engineering Failure Analysis, no. 45, pp. 204-224, 2014.

[2] M.-H. Evans, A.D. Richardson, L. Wang, R.J.K. Wood, W.B. Anderson, "Confirming Subsurface Initiation at Non-Metallic Inclusions as One Mechanism for White Etching Crack (WEC) Formation," in Tribology International, no. 75, pp. 87-97, 2014.

[3] A. Bhattacharyya, G. Subhash, N. Arakere, "Evolution of Subsurface Plastic Zone Due to Rolling Contact Fatigue of N-50 NiL Case Hardened Bearing Steel," in International Journal of Fatigue, no. 59, pp. 102-113, 2014.

[4] G. Donzella, A. Mazzù, C. Petrogalli, "Failure Assessment of Subsurface Rolling Contact Fatigue in Surface Hardened Components," in Engineering Fracture Mechanics, no. 103, pp. 26-38, 2013.

[5] A.A. Shanyavskiy, "Mechanisms and Modeling of Subsurface Fatigue Cracking in Metals," in Engineering Fracture Mechanics, no. 110, pp. 350-363, 2013.

[6] K. Zhou, R. Wei, "Modeling Cracks and Inclusions Near Surfaces Under Contact Loading," in International Journal of Mechanical Sciences, no. 83, pp. 163-171, 2014.

[7] B. Wilson, M.G. Dick, "Roller Loads and Hertzian Contact Stress Modeling in Railcar Bearings Using Finite Element Analysis," in Proceedings of the ASME RTD/TTCI Roller and Journal Bearing Symposium, Chicago, Illinois, Septemer 11-12, 2007.

[8] Y. Sandaiji, E. Tamura, T. Tsuchida, "Influence of Inclusion Type on Internal Fatigue Fracture Under Cyclic Shear Stress," in Procedia Materials Science, no. 3, pp. 894-899, 2014.

[9] M. Cerullo, "Sub-surface Fatigue Crack Growth at Alumina Inclusions in AISI 52100 Roller Bearings," in Procedia Engineering, no. 74, pp. 333-338, 2014.

[10] J. Chen, Q. Fang, Y. Liu, " Interaction Between Dislocation and Subsurface Crack Under Condition of Slip Caused by Half-plane Contact Surface Normal Force," in Engineering Fracture Mechanics, no. 114, pp. 115-126, 2013.

[11] W.A. Glaeser, S.J. Shaffer, Battele Laboratories, "Contact Fatigue," in ASM Handbook: Fatigue and Fracture, vol. 19, pp. 331-336, 1996.

[12] K. Hashimoto, T. Fujimatsu, N. Tsunekage, K. Hiraoka, K. Kida, E. Costa Santos, "Study of Rolling Contact Fatigue of Bearing Steels in Relation to Various Oxide Inclusions," in Material and Design, no. 32, pp. 1605-1611, 2011.

[13] K. Hashimoto, T. Fujimatsu, N. Tsunekage, K. Hiraoka, K. Kida, E. Costa Santos, "Effect of Inclusion/Matrix Interface Cavities on Internal-Fracture-Type Rolling Contact Fatigue Life," in Materials and Design, no. 32, pp. 4980-4985, 2011.

[14] C. Tarawneh, L. Koester, A.J. Fuller, B.M. Wilson, J.A. Turner, "Service Life Testing of Components with Defects in the Rolling Contact Fatigue Zone," in ASTM International, STP 1548, West Conshohocken, PA, pp. 67-83, 2012.

[15] C.M. Tarawneh, J.A. Turner, L. Koester, B.M. Wilson, "Service Life Testing of Railroad Bearings with Known Subsurface Inclusions: Detected with Advanced Ultrasonic Technology," in International Journal of Railway Technology, vol. 2, 2013.